

Fenton Chemistry of Fe^{III}-Exchanged Zeolitic Minerals Treated with Antioxidants

TONI A. RUDA AND PRABIR K. DUTTA*

Department of Chemistry, The Ohio State University,
100 West 18th Avenue, Columbus, Ohio 43210

Respirable mineral fibers, such as asbestos, are known to cause pleural mesothelioma, pulmonary fibrosis, and bronchial carcinoma, often years after exposure. Erionite and mordenite, two mineral aluminosilicates (zeolites) with different toxicities, can be used as models to help understand asbestos toxicity. Erionite is carcinogenic, while mordenite is relatively benign. No iron is typically present in erionite or mordenite, but because of their ion-exchange properties they can acquire iron after inhalation. The iron is typically in the Fe^{III} form and will need to be reduced prior to any Fenton activity. Lung lining fluid contains antioxidants, such as glutathione (GSH) and ascorbic acid (AA), which can reduce Fe^{III} to Fe^{II}. In this study, we have compared the Fenton reactivity of Fe^{III}-exchanged erionite and mordenite after treatment with antioxidants. The Fenton assay involved the reaction of hydroxyl radicals with dimethyl sulfoxide. Fenton reactivity was most marked with AA followed by GSH, and hydrogen peroxide also exhibited minor reactivity. Erionite generated an order of magnitude greater hydroxyl radicals than mordenite, normalized to the surface iron content, providing support for the hypothesis that the iron coordination at the mineral surface plays a significant role in bioactivity.

Introduction

The development of pulmonary fibrosis, bronchogenic carcinoma, and malignant mesothelioma has been linked to environmental and occupational exposure of mineral particulates, asbestos in particular (1, 2). Asbestos is a group of naturally occurring hydrated silicates and is comprised of six major fiber types with different chemical compositions, morphologies, and durabilities (3). The toxicity of asbestos fiber has been related to physicochemical properties such as shape, dimension, biopersistence, chemical composition, surface charge, and solubility (1, 2). Asbestos toxicity has been correlated with iron in the framework, iron that can be chelated into solution, and iron that can be complexed on the surface by silanol groups. These iron species can participate in Fenton chemistry to produce free radicals (4, 5). To determine what causes fibers to be toxic, it is important to develop relationships between surface characteristics and bioactivity.

The aluminosilicate minerals erionite and mordenite provide good models for studying bioactivity because of their contrasting toxicity. Mordenite, a natural mostly nonfibrous mineral zeolite, is known to have little biological activity (6). Erionite, a natural fibrous mineral zeolite, is known to be the

most carcinogenic fiber, more so than asbestos (7, 8). These zeolites contain little to no iron in their framework or as ion-exchangeable ions. However, since zeolites are crystalline aluminosilicates with interlinked SiO₄ and AlO₄ tetrahedral frameworks, they are capable of ion-exchange (9). The toxicity of erionite is proposed to be due to ion-exchanged iron that participates in Fenton chemistry (8, 10). A similar ion-exchange process can also occur on mordenite, which is benign, suggesting that other factors must play a role in toxicity. In a recent study, we examined reactive oxygen species formation (superoxide assay by luminol chemiluminescence) by macrophages upon phagocytosis of erionite versus mordenite and found that they were of a similar magnitude. However, the Fenton reactivities of Fe^{II}-exchanged erionite and mordenite were different, with the former showing a factor of 2 increase in hydroxyl radical production for comparable iron loading levels. We proposed that the differences in surface structure cause iron to coordinate differently, which influences the redox properties (11). We have also reported that erionite is significantly more cytotoxic and mutagenic than mordenite in the presence of Fe^{II} ions (12).

After inhalation, it is likely that the iron exchanged onto the mineral in the lung is in the Fe^{III} form and will need to be reduced prior to exhibiting Fenton reactivity. The lung has several lines of defense against inhaled minerals, including the epithelial lung lining fluid (LLF) (13, 14). When fibers interact with LLF, the surface reactivity may be modified (15, 16). Two of the main antioxidants found in LLF, ascorbic acid and glutathione, are able to reduce the surface iron of inhaled particles (17, 18). The purpose of this study is to compare the Fenton reactivity of Fe^{III}-exchanged erionite and mordenite after treatment with glutathione or ascorbic acid.

Experimental Section

Iron Incorporation into Zeolites. Iron was exchanged into the zeolites following a method adapted from previously published procedures (19, 20). Ground erionite or mordenite (1 g, Minerals Research, Clarkson, NY) was shaken for 15 min with 10 mL of 0.1 M NaCl (Aldrich, Milwaukee, WI). The grinding of the minerals was necessary to break up the agglomerates. The samples were centrifuged, the supernatant was discarded, and the process was repeated twice. A slurry was prepared with the zeolites using 5 mL of water. A solution of 0.1 M FeCl₃ (Fluka, Fairlawn, NJ) and 0.5 M KSCN (Aldrich, Milwaukee, WI) was made, and the ferric thiocyanate product was extracted with an equal volume of diethyl ether (J. T. Baker Chemical, Phillipsburg, NJ). Approximately 10 mL of the extract was added to the zeolite slurry and shaken for 60 min. The samples were washed with water and dried at 45 °C.

Zeolite Crystallinity. X-ray powder diffraction patterns were monitored with a Rigaku Geigerflex diffractometer using nickel-filtered Cu K α radiation (40 kV and 25 mA).

Surface Iron Measurements. Dab-4Br was synthesized following a method previously published (21). The first step in Dab-4Br synthesis was dissolving 0.016 mol of 1,4-diazabicyclo[2.2.2]octane (Dabco) in 16 mL of dimethyl sulfoxide and heating to 45 °C with stirring. Approximately 0.016 mol of 1,4-dibromobutane was added dropwise, and the temperature was kept below 70 °C during this step. The temperature was held at 60 °C for 1 h, then increased to 90 °C for 6 h. The solution was then cooled overnight and washed with ether, methanol, and ether once more. The solid was allowed to dry, and the product was a white/faint yellow,

* Corresponding author phone: (614) 292-4532; fax: (614) 688-5402; e-mail: dutta@chemistry.ohio-state.edu.

nontacky powder. The compound's structure was confirmed via NMR with the peaks at 2.1, 3.8, and 4.2 ppm, which matched the published data (21).

A solution of Dab-4Br was made by adding 0.5 g of Dab-4Br to 40 mL of Nanopure water. Approximately 8 mL of the Dab-4Br solution was added to 0.4 g of the zeolite and shaken for 40 h. The supernatant (1 mL) was placed in a 5 mL volumetric flask, and the pH was adjusted with 1.5 mL of a 1 M sodium acetate buffer. Approximately 1 mL of 0.03 M ascorbic acid (AA) was added, then 1 mL of 0.5 mM phenanthroline was added. The color was allowed to develop for 2 h, the solution was diluted to 5 mL, and then the absorbance at 512 nm was measured on a Shimadzu UV-2501PC spectrophotometer (Shimadzu, Columbia, MD).

Exposure of Zeolites to Antioxidants. A 10 mL portion of a 200 μ M AA (Aldrich, Milwaukee, WI) or glutathione (GSH) (Sigma-Aldrich, St. Louis, MO) solution was added to 1 g of the dried, iron-exchanged zeolite. The sample was placed on a wrist shaker for 30 min and then centrifuged. The supernatant was discarded, and 10 mL of a solution of 0.353 mM hydrogen peroxide (Fluka, Fairlawn, NJ) and 0.934 mM dimethyl sulfoxide (Acros, NJ) was added to the zeolite. The sample was placed on a wrist shaker for 1 h. The sample was then centrifuged, and the supernatant was utilized for hydroxyl radical detection.

Detection of Hydroxyl Radicals. Hydroxyl radicals were detected spectrophotometrically by a previously published procedure (22). A 2 mL portion of the supernatant from the exposed zeolite was pH-adjusted to \sim 2.5 by adding 0.3 mL of 0.01 N HCl (Fluka, Fairlawn, NJ). The supernatant then had 0.2 mL of 0.02 M Fast Blue BB dye (Fluka, Fairlawn, NJ) solution added. The 0.2 mL came from 1 mL of the Fast Blue BB dye extracted with 1 mL chloroform. Note that the Fast Blue BB dye is light sensitive. The dye reacted with the solution for 10 min in the dark, then 1.5 mL of a 3:1 toluene-butanol solution was added to stop the reaction. The solution was vortexed for 2 min, then centrifuged for 3 min. Approximately 1 mL of the upper phase was transferred to a cuvette, 2 mL of butanol-saturated water was added, and the mixture was vortexed for 30 s then centrifuged for 3 min. Approximately 0.9 mL of the upper phase was placed in a cuvette with 1.5 mL of 3:1 toluene-butanol and 0.1 mL of pyridine-glacial acetic acid. At acidic pH the color fades, so pyridine-glacial acetic acid is added to increase stability. The spectrum was recorded on a Shimadzu UV-2501PC spectrophotometer (Shimadzu, Columbia, MD) from 520 to 330 nm. The absorbance peak at 425 nm represented the diazo complex of interest. The larger peak around 320 nm is a photooxidized species from the Fast Blue BB dye. The reference was 2.4 mL of the 3:1 toluene-butanol solution. A calibration curve was previously made with methanesulfinic acid sodium salt so that known concentrations could be determined.

X-Ray Photoelectron Spectroscopy Studies of Surface Iron. X-ray photoelectron spectra were taken of Fe^{III}-exchanged mordenite and erionite with a Kratos Ultra Axis X-ray photoelectron spectrometer (Kratos Analytical, Shimadzu, Chestnut Ridge, NY). An Al K α source (1486.7 eV) was used to collect the spectrum. The analyzer was operated at a pass energy of 20 eV. The X-ray photoelectron spectroscopy sample was in pellet form. Binding energies were referenced to the Si 2p peak at 102.8 eV from the silicon(IV) in the minerals.

Results

Ion-Exchange Process. Typically, ion-exchange of zeolites is done from aqueous solutions of ions. In a previous study, we noted that iron ion-exchange of zeolite-Y with Fe^{II} led to loss of crystallinity (11). The loss of crystallinity is related to the charge on the ion-exchanging cation. A loss in zeolite crystallinity or any change in the zeolite framework will

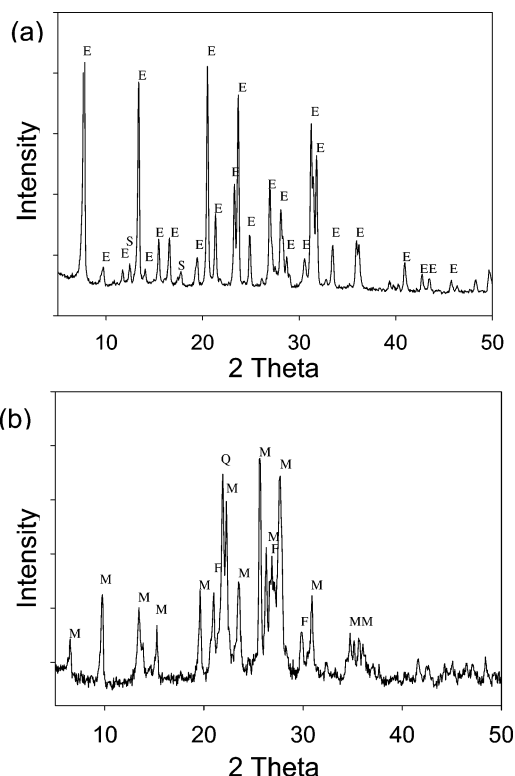
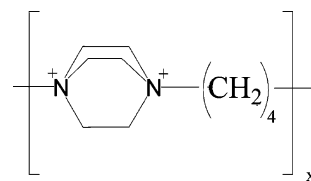


FIGURE 1. X-ray powder diffraction patterns of (a) erionite (E) with sodium aluminum silicate hydrate (S) impurity and (b) mordenite (M) with quartz (Q) and feldspar (F) impurities.

influence the Fenton reactivity. Since in the present study we are dealing with ion-exchange of a more charged iron, Fe^{III}, an alternative procedure of ion-exchange was used (20). The process involves contacting an aqueous slurry of the zeolite with an ethereal solution of Fe(SCN)_n⁽³⁻ⁿ⁾⁺. The iron thiocyanate that phase transfers into water is hydrolyzed into Fe(OH)²⁺, Fe(OH)₂⁺, Fe₂(OH)₂⁴⁺, or other polymeric species. The smaller aquated iron species rapidly ion-exchanges into the zeolite. Powder X-ray diffraction patterns of the minerals after ion-exchange (Figure 1) show no significant difference from the original X-ray diffraction patterns (data not shown), illustrating no loss in zeolite crystallinity after ion-exchange. The powder diffraction pattern for erionite matches well with the known spectra but does show a slight impurity due to sodium aluminum silicate hydrate (11). The powder diffraction pattern for mordenite indicates impurities of quartz and feldspar.

Surface Iron. Iron can ion-exchange into the porous framework as well as onto the surface. Since the reaction with AA and GSH is only occurring on the surface, it was necessary to determine the level of surface iron. The amount of surface iron present on the zeolites was estimated via ion-exchange with a cationic polymeric molecule, Dab-4Br, that will not enter the zeolites' pores because of its size. The monomeric unit of Dab-4Br is shown below. Dab-4Br is



composed of cylindrically shaped units with lengths of 8.7 Å and diameters of 6.1 Å (21). The erionite surface has a network of 8-membered rings with dimensions of 3.6 Å × 5.2 Å (23). Mordenite has 4-, 8-, and 12-membered rings, with

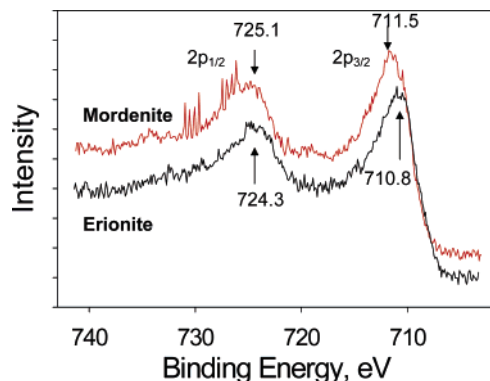
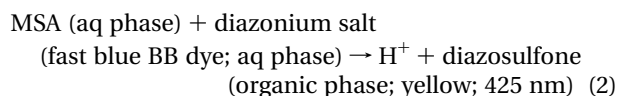
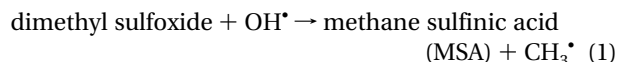


FIGURE 2. X-ray photoelectron spectra of Fe^{III}-exchanged erionite and mordenite (Fe 2p region).

the largest having dimensions of 7.0 Å × 6.7 Å (23). Therefore, Dab-4Br will only exchange with surface iron and not penetrate into the pores. The released iron was converted to an iron–phenanthroline complex and quantified via absorption spectroscopy. The amount of surface iron for mordenite and erionite were determined to be 1.8 × 10¹ and 8.8 × 10⁻¹ μg of iron per gram of zeolite, respectively. Note that these numbers cannot be directly compared with our previous study, which used ferrous ammonium sulfate solutions for ion-exchange (11).

X-ray photoelectron spectra of erionite and mordenite in the Fe 2p region are shown in Figure 2. Mordenite shows an increase in the binding energy for iron, i.e., the Fe 2p peak is at 711.5 eV for mordenite as compared to 710.8 eV for erionite.

Fenton Reactivity. The Fenton activity of the iron ion-exchanged mineral fibers involved reaction with GSH or AA, followed by treatment with hydrogen peroxide in the presence of dimethyl sulfoxide. The methane sulfonic acid that is created is converted to a diazosulfone compound and quantified by absorption spectroscopy. The overall process is outlined in reactions 1 and 2 (22).



The concentration of antioxidant was chosen to be 200 μM to simulate the typical concentration in LLF (24). Figure 3a shows the total hydroxyl radical generated, and Figure 3b shows the hydroxyl radical production normalized to the amount of surface iron. The error bars in Figure 3 are the result of two measurements. Data from Figure 3b are summarized in Table 1, along with the percent conversion of Fe^{III} to Fe^{II}, assuming a 1:1 stoichiometry between hydroxyl radical and iron. Several trends are apparent. First, for both erionite and mordenite, the amount of hydroxyl radical follows the order AA > GSH > no antioxidant. Note that in the absence of antioxidant the Fe^{III} can also be reduced to Fe^{II} by the hydrogen peroxide. Second, the surface iron normalized data show that erionite produces significantly more hydroxyl radicals than mordenite. Third, the amount of hydroxyl radical relative to the surface iron varies from about ~1% in the case of mordenite with no antioxidant added to ~106% with AA-treated erionite. Thus, in the case of erionite, all of the surface iron is being reduced by AA.

Discussion

The extreme carcinogenicity of erionite *in vivo* has been correlated with its ability to acquire iron in the lung (8). In

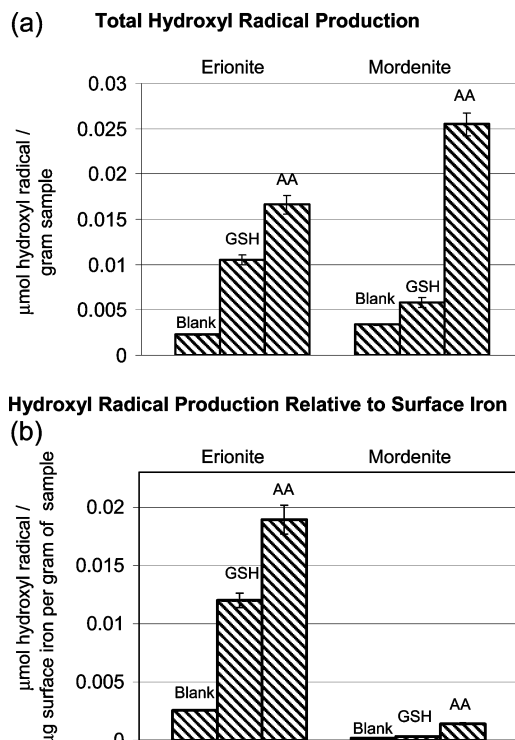
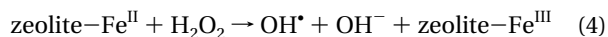
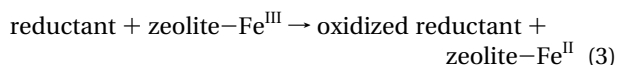


FIGURE 3. Comparison of (a) total hydroxyl radical production and (b) hydroxyl radical production normalized to surface iron in the presence of glutathione (GSH), ascorbic acid (AA), or hydrogen peroxide only (blank).

a previous study, we compared the bioactive properties of mordenite and erionite, focusing primarily on the oxidative burst upon phagocytosis by rat lung macrophages and their Fenton reactivity by an assay similar to that described in this paper (11). We found that for the same mass of mineral loading the oxidative burst increased with decreasing particle size but was relatively independent of the mineral chemical composition. However, the Fenton reactivity for erionite was higher than that of mordenite by about a factor of 2 for comparable Fe^{II} loadings. We proposed that the different mineral structures led to different surface coordination of the iron.

The fibrous nature of erionite is also relevant to its biological activity, though in this study we are focused on its surface chemistry. Typically, erionite and mordenite, with compositions (Na₂,Ca)_{3.5}K₂[Al₉Si₂₇O₇₂]·27H₂O and Na₈[Al₈-Si₁₀O₉₆]·24H₂O, respectively, contain no iron (10, 23). However, when these mineral fibers are inhaled, they can imbibe iron via ion-exchange (10). Though levels of iron *in vivo* are typically low due to sequestration by metal-binding proteins, tissue injury can lead to metal ion release (25). Bronchoalveolar lavage (BAL) has also shown the presence of chelatable and redox-active iron in the LLF (18). The iron acquired in biological systems will most likely be in the Fe^{III} form, and antioxidants present in the LLF can reduce iron, promoting Fenton reactivity as shown in reactions 3 and 4.



Considerable controversy exists regarding the mechanism of reaction 4, especially concerning the generation of free hydroxyl radicals. Alternative mechanisms propose the formation of Fe^{IV}- or Fe^V-containing species, which can act

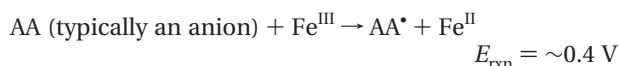
TABLE 1. Comparison of Hydroxyl Radical Production in the Presence of Different Antioxidants

	no antioxidant		glutathione		ascorbic acid	
	$\mu\text{mol OH}^{\cdot}/\mu\text{g Fe per g zeolite}$	percent conversion of Fe^{III}	$\mu\text{mol OH}^{\cdot}/\mu\text{g Fe per g zeolite}$	percent conversion of Fe^{III}	$\mu\text{mol OH}^{\cdot}/\mu\text{g Fe per g zeolite}$	percent conversion of Fe^{III}
mordenite	$1.9 \times 10^{-4} \pm 2.5 \times 10^{-6}$	1%	$3.2 \times 10^{-4} \pm 2.9 \times 10^{-5}$	2%	$1.4 \times 10^{-3} \pm 7.2 \times 10^{-5}$	8%
erionite	$2.6 \times 10^{-3} \pm 3.8 \times 10^{-5}$	15%	$1.2 \times 10^{-2} \pm 6.2 \times 10^{-4}$	67%	$1.9 \times 10^{-2} \pm 1.2 \times 10^{-3}$	106%

as the oxidants (26–29). In this study, we represent the active oxidants in Fenton chemistry as hydroxyl radicals.

Debate regarding which molecules play the role of reductant in reaction 3 exists (30, 31). The dominant antioxidants in the LLF that can reduce Fe^{III} are AA and GSH (10, 16). AA plays an important biological role as a cosubstrate in the reduction of transition metal ions for hydroxylase and oxygenase enzymes. In vitro studies have shown that AA can exhibit a pro-oxidant role in biological fluids depending on the nature of the iron complex, i.e., in the presence of iron–EDTA, but not if present as ferrous ammonium sulfate (32, 33).

Both AA and GSH can reduce iron; however, AA should be able to more easily reduce Fe^{III} .



Besides reducing Fe^{III} to Fe^{II} , AA can also react with mineral surfaces and bring about dissolution, as has been noted for silica and asbestos (10, 34, 35). Since our goal was to compare surface reactivity of erionite and mordenite, the reaction with the antioxidants was limited to 30 min, and the antioxidant was removed prior to studying Fenton reactivity. Another reason to remove the antioxidants from the system prior to the Fenton reaction was to avoid recycling the redox states of iron and the reaction of the thiol and ascorbate radicals with oxygen, which promotes additional oxy-radical mediated reactions.

As shown in Table 1, AA is more effective at promoting Fenton chemistry than GSH and hydrogen peroxide for both minerals. AA is a stronger reducing agent than GSH, since it will reduce the GSH radical, and is therefore expected to reduce a larger fraction of the zeolites' surface iron. The production of hydroxyl radical from an $\text{Fe}^{\text{II}}/\text{EDTA}/\text{H}_2\text{O}_2$ system in the presence of GSH and AA has been reported (36).

In the present study, erionite is about an order of magnitude more Fenton reactive than mordenite for all reductants, normalized to the surface iron levels. This is quite striking, especially considering that the Fenton reactivity of Fe^{II} showed only a factor of 2 increase for erionite (reaction 4) (11). The rationale for normalizing Fenton activity with respect to surface iron is that the iron present on the minerals' surface is in the molecular form as coordinated Fe^{III} . As long as the Fe^{III} is isolated, the normalized reactivity provides a direct comparison of how the different iron coordination on the two mineral surfaces is influencing the Fenton activity. Another reason for examining normalized reactivity is that all iron on the minerals was introduced via ion-exchange (i.e. no framework iron). The high Fenton activity of erionite is also consistent with the report that, normalized to the iron content, erionite was about 200 times more reactive than crocidolite for DNA single-strand breaks (8, 10).

Both natural mineral samples have impurities, quartz and feldspar for mordenite and an aluminosilicate for erionite. Are these impurities relevant in the Fenton chemistry? First, the level of impurities in erionite are quite small, as shown by the X-ray diffraction patterns in Figure 1 (impurities are

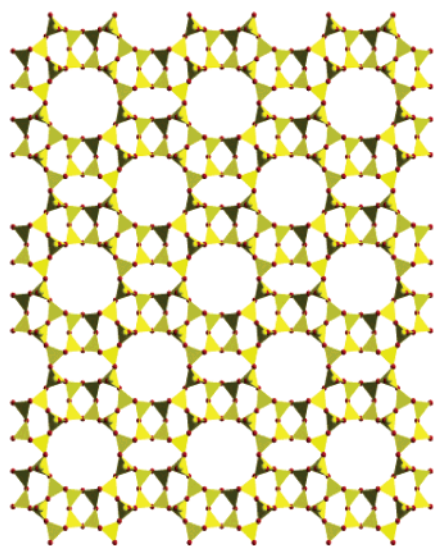
marked as "S") and thus expected to play a minor role. The major impurity in mordenite is quartz and should have a considerably lower ion-exchange binding capacity.

We are proposing that the Fenton chemistry is occurring on the surface of the minerals. After the treatment with GSH or AA, the solution is removed prior to the hydroxyl radical assay using the solid, and thus all solubilized iron is removed. The importance of surface and mobilized iron from crocidolite asbestos in hydroxyl radical generation has been noted (37–39). Asbestos toxicity has also been correlated with specific surface iron binding sites. The bioactivity of the iron is dependent on the coordination geometry (38).

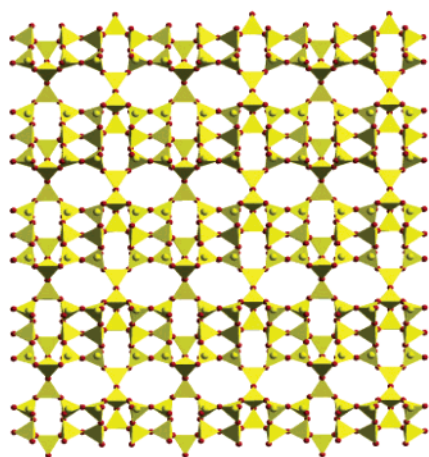
For reaction 3, the ligands determine the reduction potential of iron and will be the controlling feature for the efficacy with which reductants can reduce Fe^{III} . The ligand environment also plays a critical role in reaction 4. For an inner sphere mechanism of reaction 4, availability of ligation sites through which hydrogen peroxide can bind to Fe^{II} is necessary. For example, with ligands such as EDTA and citrate, which upon iron complexation still leave available coordination sites, the complexes are redox-active. However, strongly coordinated chelating ligands, such as desferrioxamine B and ferrozine, render the iron redox-inactive (27).

The XPS data provide some insight on the coordination environments for Fe^{III} –erionite and Fe^{III} –mordenite. For mordenite, the peaks are shifted to higher binding energies, e.g., for the $\text{Fe } 2p_{3/2}$ by 0.8 eV. The shift indicates that in mordenite the Fe^{III} is coordinated by stronger electron-withdrawing ligands. Among the minerals, the closest parallel is the comparison between Fe_2O_3 and goethite, FeOOH . The presence of hydroxyl ligands in goethite leads to increased binding energy for both $\text{Fe } 2p$ and $\text{Fe } 3p$ peaks, e.g., the $\text{Fe } 2p$ by about 0.85 eV (40). The higher metal (2p) binding energy is observed also for other metal oxides and hydroxides, such as those of copper, cobalt, zinc, and chromium (41). The possible ligands on the zeolite mineral surface are water, hydroxide, O from the T–O–T (T = Si, Al) framework, and broken T–O bonds on the surface. A simple correlation between binding energy and reducibility cannot be made because, as mentioned above, the coordination environment also determines the reduction kinetics.

Figure 4 is a surface structure rendering of mordenite and erionite showing the different rings, 4-, 5-, 8-, and 12-membered rings for mordenite and 4-, 6-, and 8-membered rings for erionite. Certainly, the coordination environment and ligands of these mineral surfaces are different, leading to different redox characteristics. "Free" metal ions are thought to be very low in vivo due to their sequestration by various metal-binding proteins. Bleomycin-detectable iron in BAL from normal humans (control) was found to be $0.132 \pm 0.019 \mu\text{mol/L}$ ($7.392 \mu\text{g/L}$), whereas total iron content in the BAL of a normal human was $0.212 \pm 0.038 \mu\text{mol/L}$ ($11.872 \mu\text{g/L}$) (18). At these low levels of iron in vivo, the amounts of iron on the minerals' surface are expected to be small, and the present study suggests that, under these circumstances, erionite will exhibit enhanced Fenton activity compared to equivalent levels of iron on mordenite.



Mordenite



Erionite

FIGURE 4. Aluminosilicate ring structures in mordenite and erionite.

The focus of this study has been to compare the Fenton reactivity of Fe^{III}-exchanged erionite and mordenite, two zeolitic minerals well known for very different toxicities upon inhalation. Since the Fenton reaction requires the presence of Fe^{II}, which most likely occurs in biological systems due to Fe^{III} reduction by antioxidants present in the LLF, such as AA and GSH, we studied the Fenton reaction of Fe^{III}-erionite and Fe^{III}-mordenite in the presence of these antioxidants. The Fenton reactivity as measured by the reaction of dimethyl sulfoxide with the hydroxyl radicals (produced from hydrogen peroxide) shows an order of magnitude increase for erionite as compared to mordenite if normalized to the amount of surface iron per gram of zeolite. The extent of Fenton reactivity increased in the order AA > GSH > no antioxidant. (Note that hydrogen peroxide was present in all cases.) The higher Fenton reactivity of Fe^{III}-erionite over Fe^{III}-mordenite must be related to the surface structure, which leads to different coordination states and therefore different redox properties.

Acknowledgments

We acknowledge funding from the NSF IGERT (Grant No. 0221678) and EMSI programs.

Literature Cited

- (1) Mossman, B. T.; Gee, J. B. L. Asbestos-related diseases. *N. Engl. J. Med.* **1989**, *320* (26), 1721–1730.
- (2) Mossman, B. T.; Bignon, J.; Corn, M.; Seaton, A.; Gee, J. B. L. Asbestos: Scientific developments and implications for public policy. *Science* **1990**, *247*, 294–301.
- (3) Veblen, D. R.; Wylie, A. G. In *Reviews in Mineralogy*; Gutherie, G. D., Mossman, B. T., Eds.; Bookcrafters, Inc.: Chelsea, MI, 1993; Vol. 28, pp 61–137.
- (4) *Mechanisms of Fibre Carcinogenesis*; Kane, A. B., Boffetta, P., Wilbourn, J. D., Eds.; IARC Scientific Publication 140; IARC: Lyon, France, 1996.
- (5) Kamp, D. W.; Weitzman, S. A. The molecular basis of asbestos induced lung injury. *Thorax* **1999**, *54*, 638–652.
- (6) Guthrie, G. D., Jr. Biological effects of inhaled minerals. *Am. Mineral.* **1992**, *77*, 225–243.
- (7) Wagner, J. C.; Skidmore, J. W.; Hill, R. J.; Griffiths, D. M. Erionite exposure and mesotheliomas in rats. *Br. J. Cancer* **1985**, *51*, 727–730.
- (8) Eborn, S. K.; Aust, A. E. Effect of iron acquisition on induction of DNA single-strand breaks by erionite, a carcinogenic mineral fiber. *Arch. Biochem. Biophys.* **1995**, *316* (1), 507–514.
- (9) Auerbach, S. M.; Carrado, K. A.; Dutta, K. B. *Handbook of Zeolite Science and Technology*; Marcel Dekker: New York, 2003.
- (10) Hardy, J. A.; Aust, A. E. Iron in asbestos chemistry and carcinogenicity. *Chem. Rev.* **1995**, *95*, 97–118.
- (11) Fach, E.; Waldman, W. J.; Williams, M.; Long, J.; Meister, R. K.; Dutta, P. K. Analysis of the biological and chemical reactivity of zeolite-based aluminosilicate fibers and particulates. *Environ. Health Perspect.* **2002**, *110*, 1087–1096.
- (12) Fach, E.; Kristovich, R.; Long, J. F.; Waldman, W. J.; Dutta, P. K.; Williams, M. V. The effect of iron on the biological activities of erionite and mordenite. *Environ. Int.* **2003**, *29*, 451–458.
- (13) Cross, C. E.; van der Vliet, A.; O'Neill, C. A.; Louie, S.; Halliwell, B. Oxidants, antioxidants, and respiratory tract lining fluids. *Environ. Health Perspect.* **1994**, *102* (10), 185–191.
- (14) Slade, R.; Crissman, K.; Norwood, J.; Hatch, G. Comparison of antioxidant substances on bronchoalveolar lavage cells and fluid from humans, guinea pigs, and rats. *Exp. Lung Res.* **1993**, *19*, 469–484.
- (15) Brown, D. M.; Roberts, N. K.; Donaldson, K. Effect of coating with lung lining fluid on the ability of fibres to produce a respiratory burst in rat alveolar macrophages. *Toxicol. in Vitro* **1998**, *12*, 15–24.
- (16) Brown, D. M.; Beswick, K. S.; Bell, K. S.; Donaldson, K. Depletion of glutathione and ascorbate in lung lining fluid by respirable fibres. *Ann. Occup. Hyg.* **2000**, *44* (2), 101–108.
- (17) Fubini, B.; Arean, O. Chemical aspects of the toxicity of inhaled mineral dusts. *Chem. Soc. Rev.* **1999**, *28*, 373–381.
- (18) Gutteridge, J. M. C.; Mumby, S.; Quinlan, G. J.; Chung, K. F.; Evans, T. W. Pro-oxidant iron is present in human pulmonary epithelial lining fluid: Implications for oxidative stress in the lung. *Biochem. Biophys. Res. Commun.* **1996**, *220*, 1024–1027.
- (19) Badran, A. H.; Dwyer, J.; Evmerides, N. P.; Manford, J. A. Ferric ion exchange and breakdown of crystalline structure in zeolites. *Inorg. Chim. Acta* **1977**, *21*, 61–64.
- (20) Evmiridis, N. P. Effect of crystal structure and percentage of ion exchange on ESR spectra of hydrated Fe(III) ion exchanged synthetic zeolites. *Inorg. Chem.* **1986**, *25*, 4362–4369.
- (21) Daniels, R. H.; Kerr, G. T.; Rollmann, L. D. Cationic polymers as templates in zeolite crystallization. *J. Am. Chem. Soc.* **1978**, *100*, 3097–3100.
- (22) Babbs, C. F.; Steiner, M. G. Detection and quantitation of hydroxyl radical using dimethyl sulfoxide as molecular probe. *Methods Enzymol.* **1990**, *186*, 137–147.
- (23) Breck, D. W. *Zeolite Molecular Sieves*; Wiley-Interscience Publication: New York, 1974.
- (24) Greenwell, L.; Moreno, T.; Jones, T.; Richards, R. Particle-induced oxidative damage is ameliorated by pulmonary antioxidants. *Free Radical Biol. Med.* **2002**, *32* (9), 898–905.
- (25) Carr, A.; Frei, B. Does Vitamin C act as a pro-oxidant under physiological conditions? *FASEB J.* **1999**, *13*, 1007–1023.
- (26) Lloyd, R. V.; Hanna, P. M.; Mason, R. P. The origin of the hydroxyl radical oxygen in the Fenton reaction. *Free Radical Biol. Med.* **1997**, *22*, 885–888.
- (27) Winterbourn, C. C. Toxicity of iron and hydrogen peroxide: The Fenton reaction. *Toxicol. Lett.* **1995**, *82/83*, 969–974.
- (28) Dunford, H. B. Oxidations of iron (II)/(III) by hydrogen peroxide: From aquo to enzyme. *Coord. Chem. Rev.* **2002**, *233/234*, 311–318.

- (29) Kremer, M. L. The Fenton reaction. Dependence of the rate on pH. *J. Phys. Chem. A* **2003**, *107*, 1734–1741.
- (30) Chaudière, J.; Ferrari-iliou, R. Intracellular antioxidants: From chemical to biochemical mechanisms. *Food Chem. Toxicol.* **1999**, *37*, 949–962.
- (31) Woodside, J. V. Antioxidants in health and disease. *J. Clin. Pathol.* **2001**, *54*, 176–186.
- (32) Winterbourn, C. C. Hydroxyl radical production in body fluids. Roles of metal ions, ascorbate and superoxide. *Biochem. J.* **1981**, *198*, 125–131.
- (33) Minetti, M.; Forte, T.; Soriani, M.; Quarissima, V.; Menditto, A.; Ferrari, M. Iron-induced ascorbate oxidation in plasma as monitored by ascorbate free radical formation. No spin-trapping evidence for the hydroxyl radical in iron-overloaded plasma. *Biochem. J.* **1992**, *282*, 459–465.
- (34) Fenoglio, I.; Martra, G.; Coluccia, S.; Fubini, B. Possible role of ascorbic acid in the oxidative damage induced by inhaled crystalline silica particles. *Chem. Res. Toxicol.* **2000**, *13*, 971–975.
- (35) Martra, G.; Tomatis, M.; Fenoglio, I.; Coluccia, S.; Fubini, B. Ascorbic acid modifies the surface of asbestos: Possible implications in the molecular mechanisms of toxicity. *Chem. Res. Toxicol.* **2003**, *16*, 328–335.
- (36) Nappi, A. J.; Vass, E. Comparative studies of enhanced iron-mediated production of hydroxyl radical by glutathione, cysteine, ascorbic acid, and selected catechols. *Biochim. Biophys. Acta* **1997**, *1336*, 295–301.
- (37) Ghio, A.; Zhang, J.; Piantadosi, C. Generation of hydroxyl radical by crocidolite asbestos is proportional to surface [Fe+3]. *Arch. Biochem. Biophys.* **1992**, *298* (2), 646–650.
- (38) Shulka, A.; Gulumian, M.; Hei, T.; Kamp, D.; Rahman, Q.; Mossman, B. T.; Mossman, B. T. Serial review: Role of reactive oxygen and nitrogen species (ROS/RNS) in lung injury and diseases. Multiple roles of oxidants in the pathogenesis of asbestos-induced diseases. *Free Radical Biol. Med.* **2003**, *34* (9), 1117–1129.
- (39) Lund, L. G.; Aust, A. E. Iron mobilization from asbestos by chelators and ascorbic acid. *Arch. Biochem. Biophys.* **1990**, *278* (1), 61–64.
- (40) McIntyre, N. S.; Zetaruk, D. G. X-ray photoelectron spectroscopic studies of iron oxides. *Anal. Chem.* **1977**, *49*, 1521–1529.
- (41) McIntyre, N. S.; Cook, M. G. X-ray photoelectron studies on some oxides and hydroxides of cobalt, nickel, and copper. *Anal. Chem.* **1975**, *47*, 2208–2213.

Received for review February 18, 2005. Revised manuscript received May 5, 2005. Accepted June 6, 2005.

ES050336E